Effect of the Different Rigidity of the Chiral Crosslinker on Phase Behaviors of Side-Chain Chiral Liquid Crystalline Elastomers

Bao-Yan Zhang, Xiao-Zhi He, Qing-Feng Liao, Qun-Hua Zhou

Center for Molecular Science and Engineering, Northeastern University, Shenyang 110004, People's Republic of China

Received 15 January 2007; accepted 22 April 2007
DOI 10.1002/app.27059
Published online 12 October 2007 in Wiley InterScience (www.interscience.wiley.com).

ABSTRACT: In the present work, the phase behaviors of two series of side-chain liquid crystalline elastomers (**PI** and **PII** series) derived from the same nematic liquid crystalline monomer and the different rigidity of chiral bisolefinic crosslinking units have been compared and studied extensively, and the effect of the different rigidity of crosslinker on the phase behavior of elastomers has been discussed. The chemical structure of the monomers and polymers obtained were confirmed by FTIR and ^{1}H NMR spectroscopy. The phase behaviors were investigated by differential scanning calorimetry, polarizing optical microscopy measurement, thermogravimetric analyses, and X-ray diffraction measurement. The two series of elastomers showed smectic or cholesteric phases. When the amount of different crosslinking units was less than 15 mol %, both of the elastomers displayed elasticity, reversible phase transition with wide mesophase temperature ranges, and high thermal stability. It is shown that the isotropization temperature values of **PII** series are higher than those of **PI** series, and the glass transition temperature values of **PII** series varied smoothly and that of **PI** series changed smoothly first and then abruptly with increasing the contents of crosslinkers with different rigidity. In addition, **PI** series showed an interesting change in LC texture near clearing point, but **PII** series did not. © 2007 Wiley Periodicals, Inc. J Appl Polym Sci 107: 1479–1486, 2008

Key words: crosslinking; elastomer; chiral smectic C; liquid crystal

INTRODUCTION

It is well known that material science is directed toward the development of multifunctional and oriented structures. Chiral liquid crystalline elastomers (CLCEs) are one of the representative research fields. CLCEs have been paid much attention since these have unique properties and potential applications in numerous areas, especially in nonlinear optical materials, electro-optical materials, fast optical switch, and piezoelectricity.[1–7] Recent theoretical and experimental studies have demonstrated that piezoelectric properties also can be obtained from cholesteric LCEs. Especially, it is worthwhile to notice that they are ideal materials for the investigation of piezoelectric effects,[8–16] because elastomers prevent macroscopic flow which disturbs the emergency of piezoelectricity in the conventional low-molar mass ferroelectric liquid crystals.[17,18] At present, chiral smectic C(S_C*) elastomers containing materials have attracted both industrial and scientific interests. Chiral smectic C(S_C*) elastomers can be obtained by combination of a chiral component and a mesogenic crosslinking unit or a mesogenic monomer and a chiral crosslinking unit. However, to the best of our knowledge, chiral smectic C and cholesteric LCEs bearing chiral crosslinking agents have few been described so far, as regarding the compared studies on elastomers with different rigidity chiral crosslinkers which have been even more little described. So it is necessary and significant to synthesize various kinds of side-chain chiral LCEs, to explore their properties and look for the optimal chiral crosslinker and reaction condition, and to be applied in effect.

Our teams have done many research works in the field of chiral LCEs. Many new kinds of crosslinkers such as nematic phase, smectic phase, and chiral have been synthesized, and the effect of the length of carbochain on chiral LCEs properties also has been studied,[19–22] which enriched the contents of LCE and offered valuable data for further application. In the present study, two series of side-chain chiral LCEs derivatized from different chiral crosslinking agents $\mathbf{M_1}$: isosorbide 4-allyloxybenzoylbisate, $\mathbf{M_2}$: isosorbide 4-undecanoyloxybisate, and nematic liquid crystalline monomer $\mathbf{M_3}$: heptyloxy-4-allyloxybiphenyl-4′-benzoate were synthesized selectively and the effects of

Correspondence to: B.-Y. Zhang (baoyanzhang@hotmail.com).
Contract grant sponsors: National Natural Science Fundamental Committee of China, Hi-Tech Research and Development Program (863) of China, China Postdoctoral Science Foundation, Postdoctoral Science and Research Foundation of Northeastern University.

different rigidity of crosslinking agent on the phase behavior of elastomers were compared to find some useful conclusion. The mesomorphic properties of the monomer and elastomers obtained were characterized by DSC, POM, TGA, and XRD.

EXPERIMENTAL

Materials

Polymethylhydrosiloxane (PMHS, M_n = 700–800) was purchased from Jilin Chemical Industry (China), Isosorbide from Yangzhou Shenzhou New Material (China), 4,4′-Biphenol from Beijing Chemical Industry (China), 3-Bromopropene from Beijing Fuxing Chemical Industry (China), Ethyloxy-benzoic acid from Shenyang Xinxi Chemical Reagent Company (China), Undecylenic acid from Beijing Jinlong Chemical Reagent (China), and 1-Bromoheptane from Yancheng Longsheng Fine Chemical Industry (China). Toluene used in the hydrosilication reaction was dried at room temperature using sodium. All other solvents and regents were purified using standard methods.

Characterization

IR spectra were measured on a Perkin Elmer Spectrum One FTIR Spectrometer (Perkin Elmer Instruments, Foster City, CA). ^{1}H NMR spectra (300 MHz) were recorded on a Varian WH-90PFT spectrometer. Specific rotation was performed with Perkin Elmer 341 polarimeter. Phase transition temperatures and thermodynamic parameters were determined by Netzsch DSC 204 (Netzsch, Germany) with a liquid-nitrogen cooling system. The thermal stability of the polymers was measured with Netzsch TGA 209C thermogravimetric analyzer. The heating and cooling rates were 10°C/min. A Leica DMRX (Leica, Germany) polarizing optical microscope equipped with a Linkam THMSE-600 (Linkam, England) hot stage was used to observe the phase transition temperatures and to analyze the LC properties for the monomers and polymers through observation of optical textures. XRD measurements were performed with a nickel-filtered Cu Kα (λ = 0.1542 nm) radiation by using a DMAX-3A Rigaku (Rigaku, Japan) powder diffractometer. The scattering vector lies in the horizontal direction and its length is defined as $q = 4\pi \sin \theta/\lambda$.

Synthesis of the monomers

The molecular formulas of monomers are shown in Scheme 1.

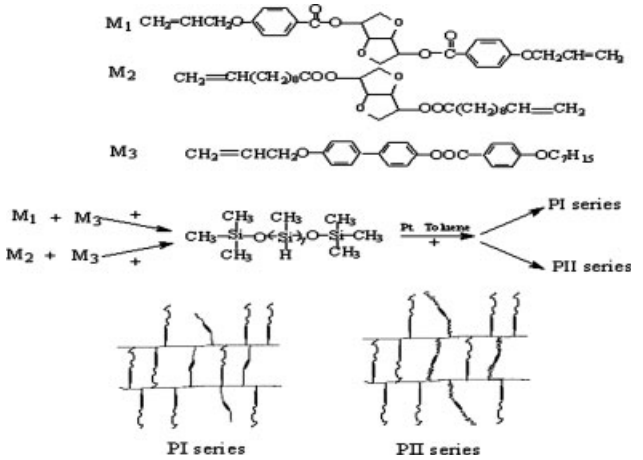

Scheme 1 Synthesis and schematic representation of **PI** and **PII** series elastomers.

Synthesis of isosorbide 4-allyloxybenzoyl bisate (M_1)

Isosorbide (0.1 mol) was dissolved in a mixture of anhydrous triethylamine (10 mL) and anhydrous chloroform (100 mL), then 4-allyloxy-benzoic acid chloride (lab synthesis) was added at room temperature, and refluxed for 72 h. The final powder product was recrystallized from ethanol. Yield: 15.8 g, 34%, mp 96°C.

$[\alpha]^{17.2}_{589} = -75.5°$, no liquid crystal properties.

IR (KBr): 3,038 (=C—H), 2,980, 2,850 (—CH_3, —CH_2), 1,716 (C=O), 1,638 (C=C), 1,605–1,450 cm^{-1} (Ar—).

^{1}H NMR ($CDCl_3$): δ 4.00–5.04 (m, 10H, isosorbide), 4.59–4.68 (d, 2H, CH_2=CHCH_2O), 5.31–5.46 (m, 2H, CH_2=CH—), 6.00–6.20 (m, 1H, CH_2=CH—), 6.92–8.06 (m, 8H, Ar—H).

Isosorbide 4-undecanoyloxy bisate (M_2)

M_2 was obtained by reaction routes similar to that of **M_1**. Extensive procedure can be found in a previously reported work.[22] Yield 65%, mp 22°C. $[\alpha]^{18.0}_{589} = +63.2°$, no liquid crystal properties.

Results are as follows.

IR (KBr): 3,057 (=CH), 2,975, 2,855 (—CH_3, —CH_2), 1,742 (C=O), 1,640 (C=C), 1,605–1,450 (Ar—), 1,235 cm^{-1} (C—O—C).

^{1}H NMR ($CHCl_3$) δ∼ (ppm): 1.29–1.66 (m, 12H, (—CH_2—)$_6$), 2.00–2.07 (d, 2H, CH_2=CHCH_2), 2.28–2.39 (m, 2H, —CH_2CH_2COO), 3.77–4.48 (m, 8H, isosorbide), 4.81–5.19 (m, 2H, CH_2=CH), 5.74–5.85 (m, 1H, CH_2=CH).

Synthesis of heptyloxy-4-allyloxy biphenyl-4′-benzoate (M_3)

4-Allyloxy-4′-hydroxy biphenyl (0.1 mol) was dissolved in a mixture of anhydrous pyridine (10 mL) and anhydrous tetrahydrofuran (100 mL), then 4-heptyloxy-benzoic acid chloride was added at once, and the reaction mixture was refluxed for 24 h. The

TABLE I
Polymerization and Solubility of Polymers PI Series

	Feed (mmol)				Solubility[b]		
Polymer	$\mathbf{M_1}$	$\mathbf{M_3}$	$\mathbf{M_1}$[a] (mol %)	Yield (%)	Toluene	Xylene	DMF
PI-1	0.000	3.500	0	86.2	+	+	+
PI-2	0.070	3.360	2	72.5	–	–	–
PI-3	0.140	3.220	4	63.3	–	–	–
PI-4	0.210	3.080	6	75.0	–	–	–
PI-5	0.280	2.940	8	59.6	–	–	–
PI-6	0.350	2.800	10	60.5	–	–	–
PI-7	0.525	2.450	15	65.3	–	–	–
PI-8	0.700	2.100	20	62.0	–	–	–

[a] Molar fraction of $\mathbf{M_1}$ based on $\mathbf{M_1}$ + $\mathbf{M_3}$.
[b] +, dissolve; −, insolubility or swelling.

cold reaction mixture was precipitated into water, the precipitated product isolated by filtration, and the flake crystal was obtained from ethanol. 4-Allyloxy-benzoic acid and 4-allyloxy-4′-hydroxy biphenyl were prepared in our laboratory.

Yield: 37.7 g, 85%, the range of liquid crystal phase is 134.3–218.8°C.

IR (KBr): 3,078, 3,038 (=C—H), 2,980–2,850 (—CH_3, —CH_2), 1,731 (C=O), 1,647 (C=C), 1,605–1,450 (Ar—), 1,258 cm^{-1} (C—O—C).

^{1}H NMR ($CDCl_3$) δ∼ (ppm): 0.88–0.93 (t, 3H, —C*H*$_3$), 1.33–1.86 (m, 10H, —C*H*$_2$—), 4.03–4.08 (d, 2H, —OC*H*$_2$—), 4.59–4.61 (d, 2H, CH_2=CHC*H*$_2$O), 5.30–5.49 (m, 2H, C*H*$_2$=), 6.00–6.20 (m, 1H, CH_2=C*H*—), 6.98–8.18 (m, 12H, Ar*H*).

Synthesis of the polymers

The synthetic ways of uncrosslinked and crosslinked polymers (elastomers) are similar and are outlined in Scheme 1. The mesogenic monomer $\mathbf{M_3}$ and the different contents of chiral crosslinking agent $\mathbf{M_1}$ reacted with Si—H of PMHS to form elastomer **PI** series in the presence of Pt catalyst. All polymers synthesized are listed in Table I. The monomer $\mathbf{M_1}$, $\mathbf{M_3}$, and PMHS were dissolved in anhydrous, freshly distilled toluene. The mixture was heated to 65°C under nitrogen and anhydrous conditions, and then 2 mL of tetrahydrofuran solution of hexchloroplatinate hydrate(IV) catalyst (5 mg/mL) was injected with a syringe. The hydrosilication reaction, which followed the track of Si—H stretch intensity up to disappearance, was completed within 30 h, as indicated by IR, followed by precipitation with methanol. The products were dried in vacuum at room temperature.

The **PII** series were synthesized by the same way using monomers $\mathbf{M_2}$, $\mathbf{M_3}$. The obtained elastomers of **PI** and **PII** series were insoluble in toluene, xylene, DMF, chloroform, etc., but could swell in these solvents. All polymers' polymerization and solubility are listed in Tables I and II.

IR (**PI** series) (KBr): 2,980, 2,850 (—CH_3, —CH_2), 1,731 (C=O), 1,605–1,450 (Ar—), 1,200–1,000 cm^{-1} (Si—O—Si).

IR (**PII** series) (KBr): 2,928–2,856 (—CH_3, —CH_2), 1,733 (C=O), 1,605–1,450 (Ar—), 1,200–1,000 cm^{-1} (Si—O—Si).

TABLE II
Polymerization and Solubility of Polymers PII Series

	Feed (mmol)				Solubility[b]		
Polymer	$\mathbf{M_2}$	$\mathbf{M_3}$	$\mathbf{M_2}$[a] (mol %)	Yield (%)	Toluene	Xylene	DMF
PII-1	0.000	3.500	0	83.2	+	+	+
PII-2	0.070	3.360	2	76.5	–	–	–
PII-3	0.140	3.220	4	73.8	–	–	–
PII-4	0.210	3.080	6	70.2	–	–	–
PII-5	0.280	2.940	8	68.5	–	–	–
PII-6	0.350	2.800	10	60.2	–	–	–
PII-7	0.525	2.450	15	65.2	–	–	–
PII-8	0.700	2.100	20	55.3	–	–	–

[a] Molar fraction of $\mathbf{M_2}$ based on $\mathbf{M_2}$ + $\mathbf{M_3}$.
[b] +, dissolve; −, insolubility or swelling.

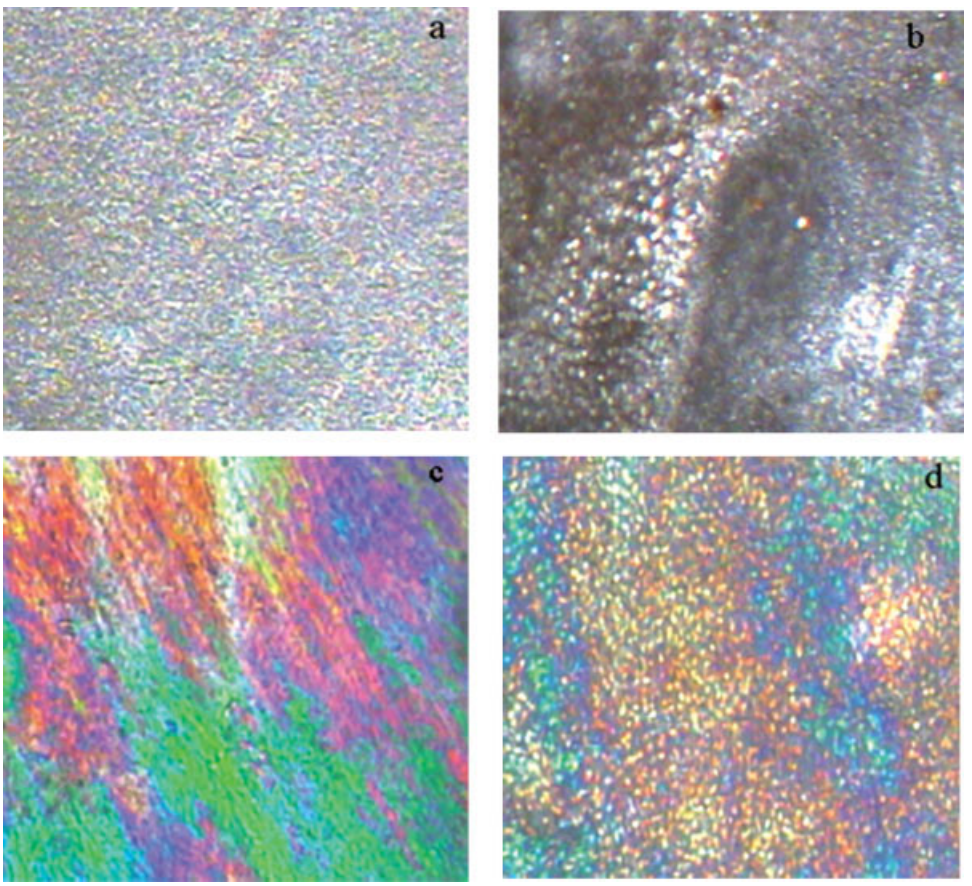

Figure 1 Optical texture of elastomers **PI** series (200×). (a) Stepped particle textures of **PI-1** at heating to 227.1°C; (b) droplet texture of **PI-1** at heating to 256.7°C; (c) lined texture of **PI-3** at heating to 159.2°C; (d) focal conic texture of **PI-3** at heating to 240.3°C. [Color figure can be viewed in the online issue, which is available at www.interscience.wiley.com.]

RESULTS AND DISCUSSION

Optical properties

Actually, POM is a preferred choice for the analysis of LC phase. It can be seen that melting point, clearing point, changes of different LC phase, and morphologic question of texture and orientate defect. The optical texture analyses of liquid crystalline monomer $\mathbf{M_3}$ and polymers **PI** and **PII** series are as follows.

The optical texture was characterized by POM with hot stage under nitrogen atmosphere. The results showed that $\mathbf{M_3}$ exhibited enantiotropic nematic phase. On heating cycle, $\mathbf{M_1}$ showed a nematic phase threaded texture; on cooling cycle, it showed a flashed droplet texture which immediately turned into threaded texture. The results suggested that $\mathbf{M_1}$ showed nematic phase on the heating cycle and the subsequent cooling cycle.

The observation revealed that the uncrosslinked polymers **PI-1**, **PII-1** (which are the same polymer) showed bright color, but the texture cannot be clearly made out. When they were heated up to the clearing point, an interesting phenomenon happened in that the strapped texture appeared at 246°C and the flashed particle at 256.7°C; the elastomers **PI-2**–**PI-6** also showed an interesting change in LC texture near the clearing points. It may be due to that the molecules have enough energy to overcome the sterically hindered effect of long rear carbochain of $\mathbf{M_3}$ and move freely and reorient at approaching to clearing point. The texture of **PI-7** did not show any change near the clearing point, which is due to the high content of chiral crosslinking agent. Elastomers **PII-2**–**PII-4** exhibited smectic stepped particle texture which is the characteristic phase of S_A or S_B phase, elastomers **PII-5**–**PII-7** exhibited lined texture which is the special texture of S_C* or cholesteric phase, and **PII** series did not show any change in LC texture near clearing point, whereas elastomers **PI-8** and **PII-8** displayed stress-induced birefringence. The representative photomicrographs of **PI**, **PII** series are shown in Figures 1(a–d) and 2(a,b), respectively. The type of LC phase of elastomers should be further characterized by X-ray diffraction.

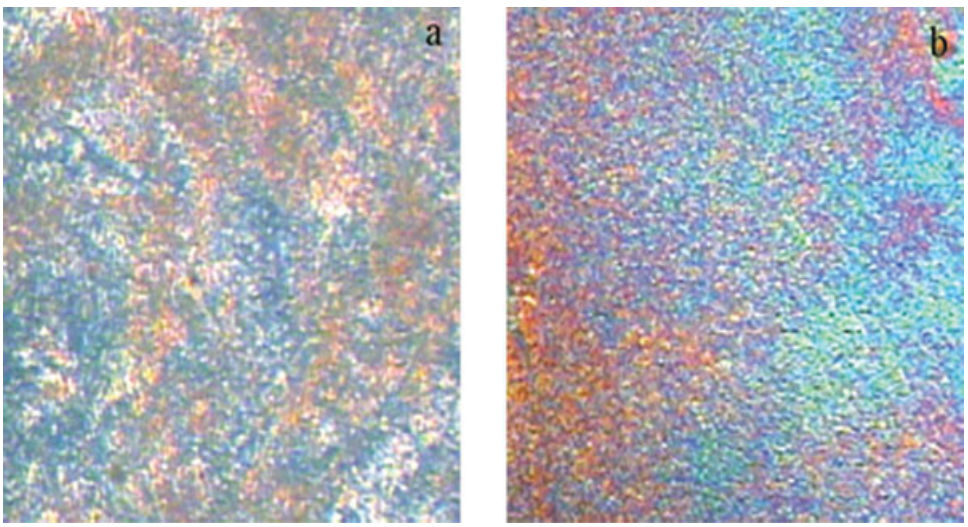

Figure 2 Optical texture of elastomers **PII** series (200×). (a) Stepped particle texture of **PII-3** at heating to 159.2°C; (b) lined texture of **PII-6** at heating to 216.9°C. [Color figure can be viewed in the online issue, which is available at www.interscience.wiley.com.]

X-ray diffraction

XRD curves of quenched representative **PI**, **PII** series are shown in Figure 3. X-ray diffraction pattern of the quenched polymer **PI-1**–**PI-6** films showed sharp reflection peaks at 2θ of 5.11–5.30 (d = 18.64–18.50 Å) and **PII-1**–**PII-7** films showed sharp reflection peak at 2θ of 5.11–5.40 (d = 18.64–18.16 Å), which were corresponding to the smectic layer spacing. The d-spacings of **PI**, **PII** series were close to or shorter than the molecular lengths of the fully stretched mesomorphic units that were calculated to be 19.09 Å. It may be concluded that the molecules were more inclined to slantwise arrange.[23,24] The films of **PI**, **PII** series showed another first sharp and then broad peaks at 2θ of 20.44–20.58° (d = 4.75–4.78 Å) and 20.44–20.75° (d = 4.75–4.81 Å) which were due to first high and then low order of the distance between the mesogenic side groups in the smectic layer. With the increasing of crosslinking agent contents, these broad peaks became weaker, which is simply related to the difference between the intrachain scattering of the mesogenic repeat and the crosslinking unit. Combining polarizing microscopy with X-ray diffraction measurements may reveal that polymers **PI-1**, **PII-1** were smectic B phase, elastomers **PI-2**–**PI-6** were chiral smectic C phase, and elastomer **PI-7** was cholesteric phase, while elastomers **PII-2**–**PII-4** were smectic A phase, elastomers **PII-5**–**PII-7** were chiral smectic C phase, and elastomers **PI-8**, **PII-8** displayed stress-induced birefringence.

It can be seen that elastomers **PI** were chiral smectic or cholesteric phase LC and elastomers **PII** series were chiral smectic phase which are due to the long carbon chain slantwise arrangement of $\mathbf{M_2}$ and $\mathbf{M_3}$. The LC texture of **PI** series changed from Chiral Smectic C to Cholesteric phase, while that of **PII** series changed from Smectic A or B to Chiral Smectic C. It is showed that the helicity of **PI** series, which owned short and rigid crosslinkers, appeared quickly, while that of **PII** series, which owned long and flexible crosslinkers, turned slowly when the length and flexibility reached a critical content. Short and rigid crosslinker can conform to the rearrangement of $\mathbf{M_3}$, while long and flexible crosslinker cannot, and so **PI** series showed an interesting change in LC texture near the clearing point, but **PII** series did not.

Thermal properties

The phase behavior of LC polymers may be readily evaluated using DSC, which provides an effective measurement of the energy required to raise the temperature as a function of temperature. Thermal properties of polymers $\mathbf{P_1}-\mathbf{P_8}$ of **PI** and **PII** are sum-

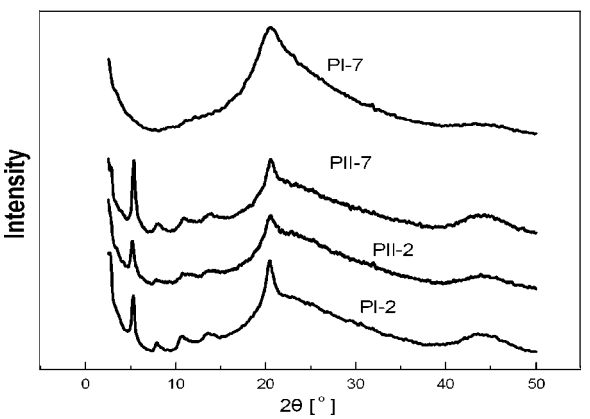

Figure 3 X-ray diffraction patterns of quenched samples.

TABLE III
Thermal Properties of Polymers PI Series

Polymer	T_g (°C)	T_i (°C)	ΔT[a]	T_a[b] (°C)
PI-1	90.0	244.0	154.0	340.6
PI-2	107.1	252.0	144.9	386.9
PI-3	98.1	241.3	143.2	385.0
PI-4	83.9	227.9	144.0	392.4
PI-5	87.6	218.0	130.4	394.5
PI-6	87.9	207.7	119.8	389.0
PI-7	74.7	188.6	113.9	386.8
PI-8	79.3	–	–	381.5

[a] Mesophase temperature ranges ($T_i - T_g$).
[b] Temperature at which the 2% weight loss occurred.

marized in Tables III and IV; representative DSC curves of **PI** and **PII** series are shown in Figure 4. The effect of different chiral crosslinkers content on phase transition temperature of the elastomers **PI** and **PII** series is shown in Figure 5.

As seen from the data of Tables III and IV and Figure 5, the general tendency of elastomers **PI** and **PII** series is basically accordant. The glass transition temperature (T_g) values of elastomers **PI-1**–**PI-6** and **PII-1**–**PII-8** fluctuated: increased, decreased, increased with the increase of the content of chiral crosslinking agent, which is due to the effect of the different acting forces between intermolecules. But the T_g values of elastomer **PI-7** abruptly changed and mismatched the common rule.

The factors influencing T_g are the properties of polymer backbone, the rigidity of mesogenic unit, the rigidity of crosslinker (ℓ_c), the content of crosslinking agent (ρ_x), and the intermolecular force due to the sterical hinder (f_s). As to the elastomers, the crosslinking agent usually plays a main role, but sometimes ℓ_c, ρ_x, and f_s cannot be omitted. When the last three factors are taken into account, the glass-transition temperature (T_g) is given by

$$T_g = T_{g0} \pm K_x \rho_x \pm f_s \quad (1)$$

TABLE IV
Thermal Properties of Polymers PII Series

Polymer	T_g (°C)	T_i (°C)	ΔT[a]	T_a[b] (°C)
PII-1	90.0	244.0	154.0	359.6
PII-2	92.9	251.4	158.5	363.8
PII-3	94.7	245.5	150.8	356.7
PII-4	85.5	240.9	155.4	349.7
PII-5	85.3	237.1	152.4	357.9
PII-6	86.4	225.8	139.4	353.9
PII-7	87.1	204.0	116.9	354.0
PII-8	92.3	–	–	347.1

[a] Mesophase temperature ranges ($T_i - T_g$).
[b] Temperature at which the 2% weight loss occurred.

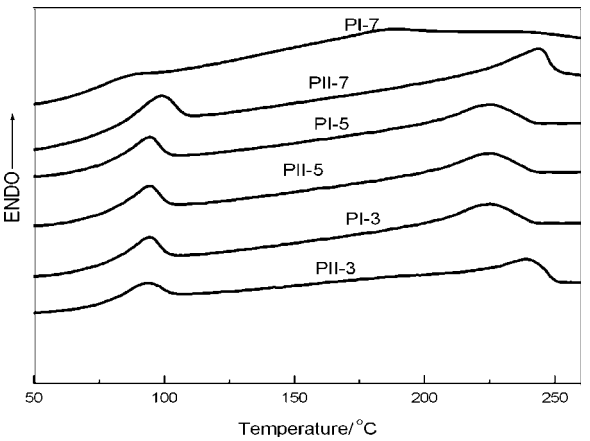

Figure 4 DSC thermographs of liquid crystalline elastomers **PI** and **PII** series (second heating).

$$T_g = T_{g0} + K_s \ell_c \pm f_s \quad (2)$$

$$T_g = T_{g0} - K_s \ell_c \pm f_s \quad (3)$$

where T_g and T_{g_o} are the glass transition temperatures of the crosslinked and uncrosslinked polymers, and K_x, K_s are constants. When the **PI** and **PII** series were studied separately, the term K_s, ℓ_c should be omitted, and eq. (1) would be used. Crosslinking has opposite effect on the properties of glass transition temperature (T_g). On one hand, the crosslinking effect which imposed additional constrains on the segment motions of polymer chains might be expected to raise the T_g temperature, on the other hand, flexible crosslinking chain which may have the influence as plasticity to reduce T_g values and f_s also has two opposite actions to T_g values; all the factors interacted and T_g values lifted by turns as a result. When comparing the properties of elastomers **PI** and **PII** series, the term $K_x\rho_x$ should be ignored, and eqs. (2) and (3) would be put into use.

Similarly, the different rigidity of the crosslinker has two opposite effects on the properties of LCEs. One is the sterically hindered effect that may increase the T_g values, the other is the plasticity that can reduce the T_g values. In the present study, the molecular lengths of $\mathbf{M_1}$, $\mathbf{M_2}$, and $\mathbf{M_3}$ are 23.02, 30.52, and 25.08 Å, respectively. It can be seen that the flexible carbochain of $\mathbf{M_3}$ moves freely in the elastomers **PII** series, and the change of f_s is small. When the flexible carbochain of $\mathbf{M_3}$ is crimped slightly in the **PI** elastomers, it may generate a large hindering effect between intermolecules and the change of f_s is large.

It can be seen that T_g values of **PI-1**–**PI-3** were higher than that of **PII-1**–**PII-3** which is due to the rigidity of $\mathbf{M_1}$ and f_s. With increasing of the contents of crosslinkers, the T_g values of **PI-4**–**PI-6** were close

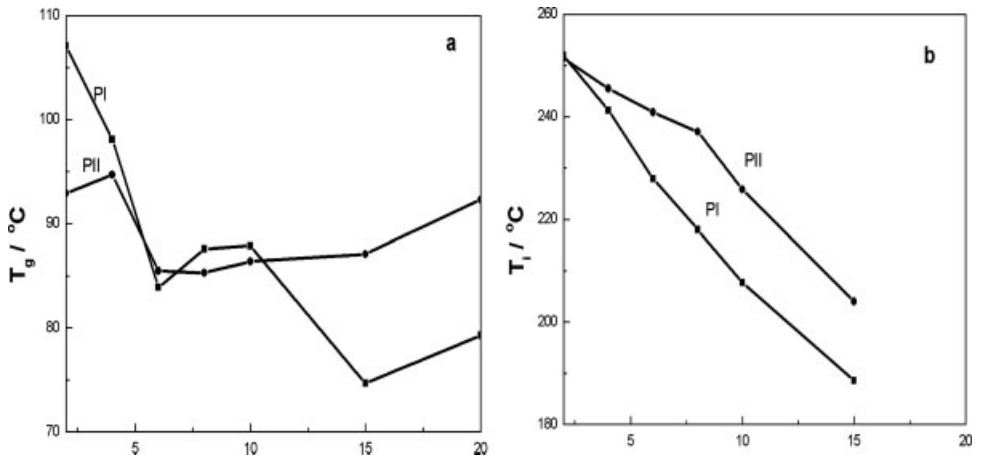

Figure 5 Effect of different chiral crosslinkers on T_g (a) and T_i (b) values of the elastomers **PI** and **PII** series.

to that of **PII-4**–**PII-6**, which was due to the equilibrium of the intermolecular force. When the crosslinker contents of **PI** series were up to 15%, the T_g values showed an abnormal phenomenon with decreasing abruptly. Under such an equivalent condition of intermolecular force, the T_g value did not increase, but reduced, which is due to the action of $\mathbf{M_3}$ flexible side chain. When increasing the crosslinker content, the contents of $\mathbf{M_3}$ would be decreased and the intermolecular action of long crimped side-chain substituent of $\mathbf{M_3}$ would be cut down. As a result, f_s decreased abruptly and the movement of $\mathbf{M_3}$ would be strengthened and the T_g value changed suddenly. When the action of crosslinking was in a leading role again, the T_g value of **PI-8** rose again, but the value is also lower than that of **PII-8**. It can be seen that the effect of f_s cannot be ignored.

Similar to T_g, crosslinking may influence the clearing point (T_i) in two ways. First, crosslinking units may act as a nonmesogenic diluent and lead to downward shift of the clearing point as increasing contents are added to a LC polymer. Second, for a long and flexible crosslinker, heating to the isotropic state required additional energy to distort the polymer backbone from the anisotropic state at crosslinking and leads to forward shift in the clearing point with increasing contents of chiral crosslinkers. It can be seen from Tables III and IV that the T_i values of **PI** and **PII** series decreased with the content of crosslinkers and the T_i values of **PII** series were higher than that of **PI** series.

At the same time, it can be seen from Tables III and IV that $\mathbf{P_1}$–$\mathbf{P_7}$ of **PI** and **PII** displayed wide mesophase temperature ranges (ΔT). ΔT values of **PI** and **PII** decreased with increasing the content of crosslinking agent. Temperatures at which 2% weight loss occurred (T_d) were greater than 350°C for **PI** and **PII** series, which reveals that the synthesized elastomers had a high thermal stability.

In addition, the optical rotations of $\mathbf{M_1}$, $\mathbf{M_2}$ were opposite, but this has little effect on the properties of chiral LCEs, because the left and right handed only have difference on the direction of optical rotation, not on helicity.

CONCLUSIONS

In this study, two series of new side-chain chiral smectic LCEs were synthesized by reacting the different chiral crosslinking agents with the same nematic monomer. The properties of the two series of new chiral side-chain smectic LCEs were characterized by DSC, TGA, POM, and XRD. Liquid crystalline phase of elastomers **PI** series changed from S_B, S_C* to cholesteric and that of elastomers **PII** series changed from S_B to S_A and then S_C* with the increasing of the content of the chiral crosslinker. It showed that the helicity of short and rigid crosslinkers appeared quickly, while that of long and flexible crosslinkers appeared slowly when it reached critical contents. Elastomers **PI** series showed an interesting change in LC texture near the clearing point, but elastomers **PII** series did not. The T_i values of **PII** series are higher than those of **PI** series and T_g values of **PII** series varied smoothly and that of **PI** series changed smoothly first and then abruptly and the f_s effect cannot be ignored. All of the obtained polymers showed very wide mesophase temperature ranges and high thermal stability.

References

1. Zentel, R. Angew Chem Adv Mater 1989, 101, 1437.
2. Zentel, R.; Reckert, G. Makromol Chem 1986, 187, 1915.
3. Loffler, R.; Finkelman, H. Macromol Chem Rapid Commun 1990, 11, 321.
4. Meier, W.; Finkelman, H. Condens Matter News 1992, 1, 15.
5. Davis, J. J Mater Chem 1993, 3, 551.

6. Mitchell, R.; Davis, J. Polymer 1987, 28, 639.
7. Broer, D. J.; Heynderickx, I. Macromolecules 1990, 23, 2474.
8. Lub, J.; Broer, D. J.; Hikmet, R. A. M.; Nierop, K. G. J. Liq Cryst 1995, 13, 319.
9. Hiraoka, K.; Finkelmann, H. Macromol Chem Phys 1995, 196, 3197.
10. Plate, N. A. R.; Talroze, R. V.; Freidzon, Ya. S.; Shibaev, V. P. Polym J 1987, 19, 135.
11. Lehmann, W.; Leister, N.; Hartmann, L.; Finkelmann, H. Mol Cryst Liq Cryst 1999, 328, 437.
12. Thomas, P.; Kurschner, K.; Strohriegl, P. Macromol Chem Phys 1999, 200, 2480.
13. Broer, D. J.; Lub, J.; Mol, G. N. Nature 1995, 378, 467.
14. Maxein, G.; Mayer, S.; Zentel, R. Macromolecules 1999, 32, 5747.
15. Goodby, J. W.; Leslie, T. M. Mol Cryst Liq Cryst 1984, 110, 175.
16. Hikmet, R. A. M.; Kemperman, H. Nature 1998, 392, 476.
17. Brand, H. Makromol Chem Rapid Commun 1989, 10, 441.
18. Hiraoka, K.; Stein, P.; Finkelmann, H. Macromol Chem Phys 2004, 205, 48.
19. Zhang, B. Y.; Hu, J. S.; Jia, Y. G.; Du, B. G. Macromol Chem Phys 2003, 204, 2123.
20. Jia, Y. G.; Zhang, B. Y.; Tian, M.; Wei, K. Q. React Funct Polym 2005, 63, 55.
21. He, X. Z.; Zhang, B. Y.; Hu, J. S.; Tian, M. Liq Cryst 2005, 32, 299.
22. He, X. Z.; Zhang, B. Y.; Sun, Q. J.; Lu, H. W.; Li, L. Liq Cryst 2005, 32, 431.
23. Sapich, B.; Stumpe, J.; Krawinkel, T.; Kricheldorf, H. R. Macromolecules 1998, 31, 1016.
24. Zhou, Q. F.; Wang, X. J. Liquid Crystal Polymer; Science Press: Beijing, 1999; p 83, 104.